Proceedings of the ASME 2016 Dynamic Systems and Control Conference
DSCC2016
October 12-14, 2016, Minneapolis, Minnesota, USA

DSCC2016-9803

CHARACTERIZATION OF RESONANT MASS SENSORS USING INKJET DEPOSITION

Nikhil Bajaj, Jeffrey F. Rhoads, and George T.-C. Chiu*
School of Mechanical Engineering, Ray W. Herrick Laboratories, and Birck Nanotechnology Center
Purdue University
West Lafayette, IN 47907
Contact Email: gchiu@purdue.edu

ABSTRACT

Micro- and millimeter-scale resonant mass sensors have received widespread research attention due to their robust and highly-sensitive performance in a wide range of detection applications. A key performance metric associated with such systems is the sensitivity of the resonant frequency of a given device to changes in mass, which needs to be calibrated for different sensor designs. This calibration is complicated by the fact that the position of any added mass on a sensor can have an effect on the measured sensitivity, and thus a spatial sensitivity mapping is needed. To date, most approaches for experimental sensitivity characterization are based upon the controlled addition of small masses. These approaches include the direct attachment of microbeads via atomic force microscopy or the selective microelectrodeposition of material, both of which are time consuming and require specialized equipment. This work proposes a method of experimental spatial sensitivity measurement that uses an inkjet system and standard sensor readout methodology to map the spatially-dependent sensitivity of a resonant mass sensor – a significantly easier experimental approach. The methodology is described and demonstrated on a quartz resonator and used to inform practical sensor development.

*Address all correspondence to this author. This work was supported by the U.S. Department of Homeland Security's Science and Technology Directorate, Office of University Programs, under Award 2013-ST-061-ED0001.

INTRODUCTION

Microscale devices lend themselves towards sensing applications due to the high sensitivity of their mechanical behavior to changes in system parameters (such as mass, stiffness, or damping), boundary conditions and various external fields. The promise associated with this high sensitivity has motivated the development of resonant sensors suitable for general mass sensing [1–6], as well as chemical and biological sensing [7–18]. As a specific example, prior art exists wherein resonant microscale sensors are used to detect explosive materials [19–22].

One of the most important metrics associated with the performance of a resonant mass sensor is the sensitivity of the resonant frequency of the device to an addition or subtraction of mass, measured in Hz/pg or equivalent units. An added mass may have more or less "effective mass" with respect to its effect on the frequency response of a resonator depending on where it is located relative to the vibrational modes of the device. Accordingly, the mass sensitivity of a resonator is spatially-dependent. This metric can be estimated in many cases via simulation or analysis. However, with complex resonator geometries or material behavior this can become difficult. In addition, even if the spatially-distributed mass sensitivity can be estimated, it is useful to be able to validate such metrics experimentally. Dohn et al. [23,24] have demonstrated this by using an etched tungsten tip to load polystyrene microbeads and magnetic microbeads with diameters of 2 μm and 2.8 μm (and masses of 4.4 pg and 14.9 pg), respectively, on various devices and estimating localized mass sensitivity through experimentation. Likewise, Wagonner et al. [25] considered the use of selectively-placed gold dots on

cantilevers and examined the effect that etching the dots away had on the sensors' frequency responses. This approach allowed for very small test masses (approximately 400 fg) but required the researchers to fabricate and test many devices. Nieradka et al. [26] approached the problem of validating mass change and position determination using focused ion beam (FIB) milling and deposition. However, this work, like those noted above, focused on beam-like device geometries.

For plate-like devices, tuning forks, or other more complex structures, a second dimension becomes important for deciding optimal placement of functional compounds and masses. Concretely, the desired outcome is to experimentally produce the differential mass sensitivity:

$$S(x_m, y_m) = \frac{\partial f(x_m, y_m)}{\partial m} \tag{1}$$

where f is a resonant frequency of a device, m is mass, $S(x_m, y_m)$ is a function with units of Hz/(unit mass), and x_m and y_m are the spatial coordinates of a small added mass. Notably, Hillier and Ward [27] used an electrochemical deposition technique with a scanning stage and microelectrode to position and deposit copper on a quartz crystal microbalance (QCM) device, and used this method to generate a 2-dimensional map of differential sensitivity.

Inkjet printing is a known method for applying functional and polymer materials to microscale devices [28–31]. It is also used in other circumstances to aerosolize compounds [32]. With inkjet printing, drop size control can be made repeatable and reliable, if the correct material and nozzle are chosen [33]. The chief contribution of this work is the development and application of an inkjet deposition-based method suitable for characterizing the spatially-dependent sensitivity of resonant mass sensors. The proposed approach is to estimate $S(x_m, y_m)$ by using a precision inkjet deposition system constructed for device functionalization. This is advantageous because the system designed for functionalizing a mass or chemical sensor can also be used to calibrate it and map its sensitivity. Precisely controlled drops can be deposited accurately using the inkjet system and allowed to dry so that the solvent in the ink evaporates and an inert material dissolved in the fluid is left as a deposit. The resulting change in resonant frequency can then be evaluated. The experimental techniques employed herein are described in the Methodology section, and the corresponding results are interpreted in the Results and Discussion section. The work concludes with a brief overview and suggestions for research extensions.

METHODOLOGY

Experimental Setup

The custom deposition system comprised of an X-Y motion stage (Anorad-XKY-C-150-150-AAA0 stage controlled by an Anorad-CM-2 controller) and a custom mounted HP (Hewlett-Packard) thermal inkjet picojet system, with printing commands provided through in-house software. An aqueous Canon thermal inkjet printing ink was used as the deposition material. The designed drop weight for aqueous inks for the selected nozzle was 28 ng, with the corresponding solids loading per drop being 6 ng.

Because aqueous inks can have a long drying time, a temperature-controlled hot air tool was used to dry the drop on the sensor. This hot air tool (normally used for hot air soldering rework) was set to 100° C and allowed to run at 50% of its maximum fan speed for 5 to 10 s at a time.

An Edmund Optics EO-1312 Color USB 3.0 Camera mounted with a 2X primary magnification, 65 mm working distance compact telecentric lens was used for imaging the sensor (with a 2.63 μm/pixel resolution) to determine drop placement locations. For the experiment conducted here, the resonant sensor was characterized using a circuit based on two Texas Instruments LMH6609 amplifiers, with one configured as a drive amplifier for the crystal and the other configured as a transimpedance amplifier with a 2 pF capacitor in parallel with a 43 Ω resistor in the feedback path. The circuit was excited and measured using a Zurich Instruments HF2LI lock-in amplifier, which had phase-locked loop (PLL) functionality. A schematic of the entire experimental system can be seen in Figure 1.

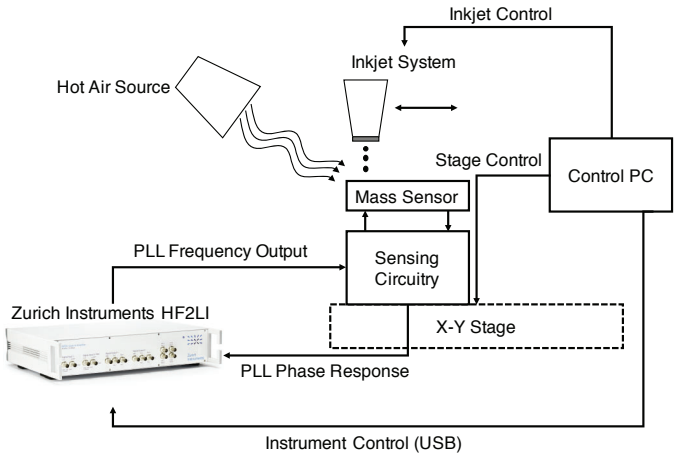

FIGURE 1. Schematic of the deposition system, including hot air source, sensing system, inkjet system, and X-Y stage positioning system.

Experimental Procedure

The CX3225 resonator is a 16 MHz member of a quartz crystal family produced by Kyocera. While the intended use of the device is as part of a crystal oscillator circuit for clock signal

generation, the device is under investigation for use in mass sensing applications due to its small size and surface mount packaging (3.2 mm by 2.5 mm). Internally, the device is a bulk-acoustic wave crystal operating in the fundamental thickness shear mode, mounted to a ceramic substrate. The experimental procedure consisted of decapping a new CX3225 resonator in order to make it accessible for inkjet printing and mass sensing. A CX3225 sensor in this state is shown in Figure 2. An initial frequency sweep was performed using the HF2LI amplifier. The results of the frequency sweep can be seen in Figure 3. Based on the results of this frequency sweep, the magnitude and phase of the response at resonance were identified, and the phase was used to allow the PLL to adjust the frequency input to the resonator and track resonance. The corresponding modulator settings, output frequency, and phase error were continuously recorded with a sampling rate of 55 Hz. The PLL loop parameters (proportional and integral) were tuned using the Zurich Instruments ziControl PLL advisor software.

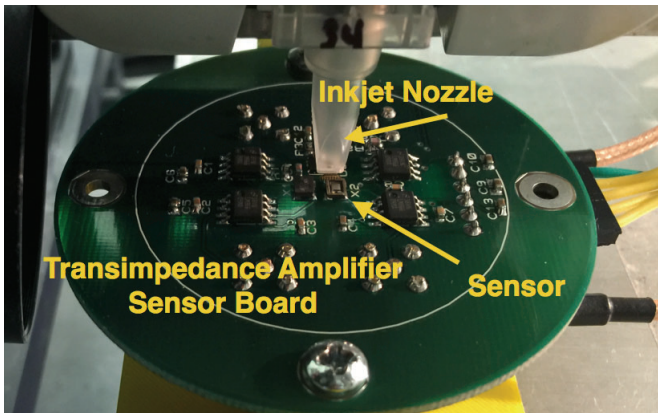

FIGURE 2. A mass sensor (with measurement circuitry) undergoing the characterization procedure.

After the PLL was configured to track the resonant frequency, the experiment continued into the iterative deposition phase. First, the inkjet deposition system was commanded to print an array of 30 drops onto a "sacrificial" substrate, a small piece of absorbent paper. It was then immediately commanded to print a single drop at a location on the resonator. The X-Y stage then moved the resonator directly in the viewing area of the downward-looking camera system and imaged the deposited drop, saving the microscope image for later use. As a pair of examples, Figure 4 shows the first drop deposited in a 51 drop experiment, and Figure 5 shows the camera image taken after the

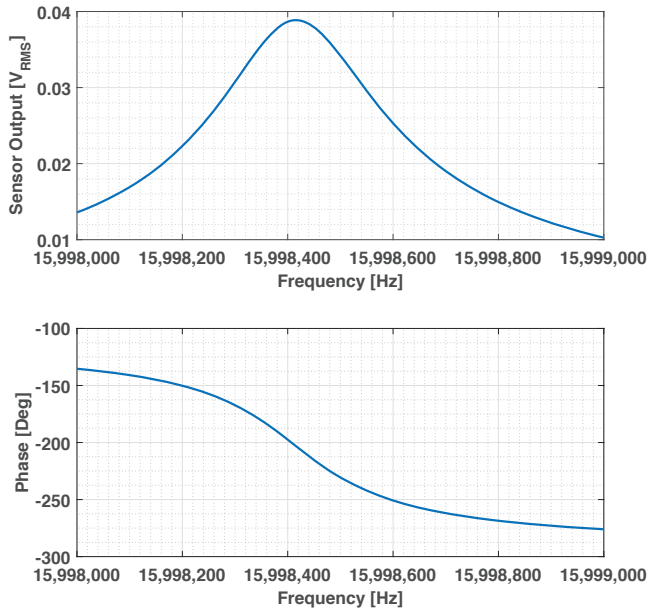

FIGURE 3. Frequency response of the 16 MHz CX3225 device prior to any ink deposition, from which f_0 can be identified.

51st drop was deposited.

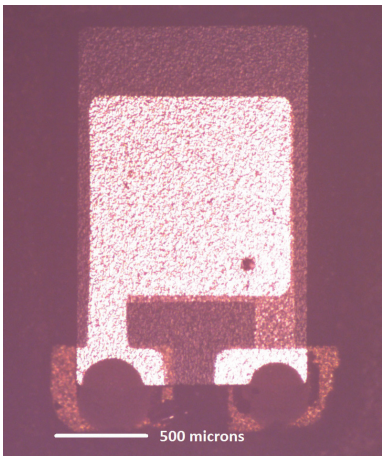

FIGURE 4. A Kyocera CX3225 device with a single drop of black inkjet ink deposited.

After each drop was deposited, the hot air tool was turned on for 5 to 10 s in order to quickly dry the droplet. The resonator was then allowed 3 to 5 min to return to thermal equilibrium before continuing with the next drop and repeating the process while

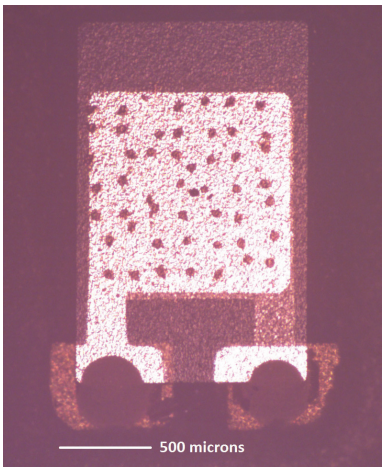

FIGURE 5. A Kyocera CX3225 device with a 51 drops of black inkjet ink deposited.

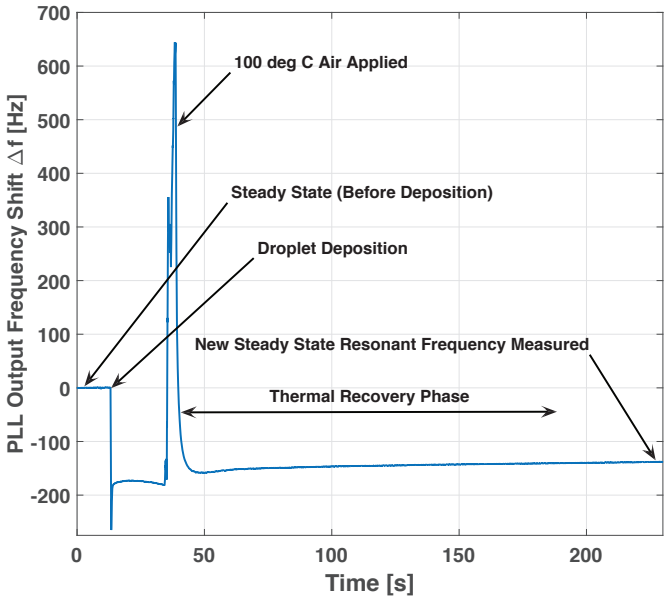

FIGURE 6. Process for a single drop deposition, with response phases identified. The shift Δf for this deposition is computed from the beginning of the single drop deposition.

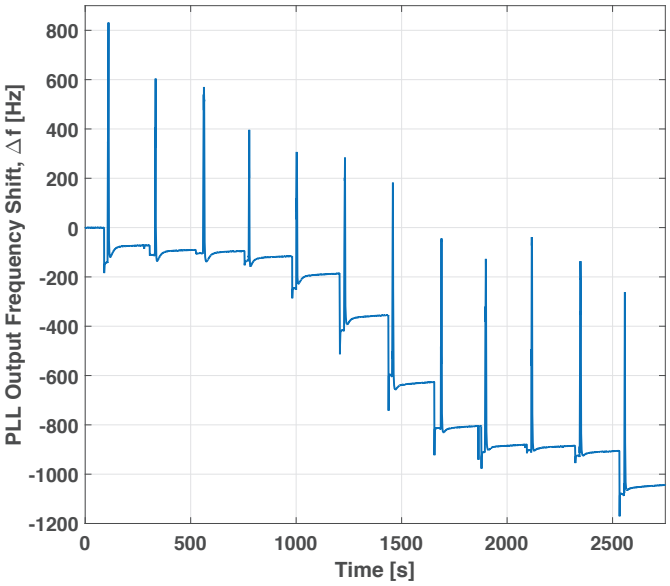

FIGURE 7. A 12 drop portion of a deposition experiment. The shift Δf is the total shift from the beginning of the deposition experiment.

adjusting the printing position of the droplet. The process for a single drop can be seen in the PLL frequency present in Figure 6, and a set of 12 subsequent drops in Figure 7. The added mass due to the drop solids content that did not evaporate during the drying stage is spread out in a "spot". In this this experiment, the deposited drop forms an approximately 55 to 65 μm diameter spot on the resonator. This spot size could potentially be further reduced by a change in nozzle diameter, printing parameters (such as back-pressure, inkjet drive voltages and pulse shaping), ink formulation changes, or potentially a change to another type of inkjet printing. However, for a device of this size, the spot size was deemed sufficiently small.

One consideration that is based on the design and behavior of the device to be evaluated is that the deposition of previous droplets in a sequence might change the sensitivity of the device to subsequent drops. In order to be sure that this is not the case, it is advisable to estimate the effect of each droplet on the sensitivity of the sensor. The device to be characterized in this work is a Kyocera CX3225 16 MHz bulk-mode resonator that shares some characteristics with QCM devices – therefore the Sauerbrey equation can be used to recover a rough estimate of average sensitivity across the device. For other geometries or types of device some estimate of sensitivity and effective mass should exist in order to ascertain whether previous mass depositions will result in significant deviation in the sensitivity of subsequent ones.

Validation of Proposed Approach for a Bulk Resonator

The Sauerbrey equation can be considered as a starting point for validation of the approach adopted herein [27,34]. This equation stipulates that for a change in mass Δm, the corresponding frequency shift can be written as

$$\Delta f \approx \frac{-2f_0^2 \Delta m}{A\sqrt{\rho_q \mu_q}} = C_f \Delta m \tag{2}$$

Here, C_f is the average sensitivity across the device, Δf is the resulting frequency shift, f_0 is the resonant crystal frequency in Hz, Δm is the mass change, A is the piezoelectrically active area, ρ_q is the density of quartz (2.648 g/cm^3) and μ_q is the the shear modulus ($2.947 * 10^{11}$ dyne/cm^2 for AT-cut quartz.) Letting $K = A\sqrt{\rho_q \mu_q}$, the differential mass sensitivity is approximately

$$S_0 = \frac{\Delta f}{\Delta m} \approx -2\frac{f_0^2}{K} \tag{3}$$

In order to determine the impact of additional drops on the mass sensitivity, let f_i be the natural frequency after the addition of i drops. Then,

$$\begin{aligned}
f_0 &= f_0, \\
\Delta f_1 &= \frac{\Delta f_0}{\Delta m}\Delta m = -\frac{2f_0^2}{K}, \\
f_1 &= \Delta f_1 + f_0, \\
\Delta f_2 &= \frac{\Delta f_1}{\Delta m}\Delta m = -\frac{2f_1^2}{K}, \\
f_2 &= \Delta f_2 + f_1, \\
&\text{etc}\ldots
\end{aligned}$$

This calculation was performed for Δm = 6000 pg, f_0 = 16 MHz, A = 0.01 cm^2, the aformentioned ρ_q and μ_q values, and iterated for 250 drops. The results can be seen in Figure 8. It appears from the plot that the trend is linear, but it is not (as the equations suggest). However, it is close to linear in the region and parameter space plotted. Nonlinear behavior of the model becomes more evident if drop mass is significantly increased, but such changes also push outside the applicability of the Sauerbrey model. Another limitation to note is that the Sauerbrey model is only valid for masses covering the entire electrode surface, so this iterated model can be considered to be a spatially-averaged model. A third limitation of the Sauerbrey model derivation is that a key assumption is that the material added has a similar stiffness and composition to the resonator material itself, which is not the case when depositing inkjet ink, so the results should only be taken as an approximation. Despite the noted limitations, the results indicate that over 100 inkjet drops, the resulting change in the differential sensitivity measurement would be $\leq 0.5\%$, which is relatively small compared to our resolution in frequency measurement and small compared to normal variations in inkjet drop volume (up to 5%) and will not make a significant difference for the sensitivity estimation accuracy.

RESULTS AND DISCUSSION

To compute the drop-to-drop frequency shift, 10 seconds of PLL output frequency data at the beginning and end of each drop response (as in Figure 6) were used. The frequency over the 10 seconds was averaged, and the drop frequency shift was computed as $\Delta f_i = f_i - f_{i-1}$. In order to correlate the ith drop with its position, the drops were identified by a MATLAB script that allowed the user to sequentially specify drop locations on the final image (with the full number of spots). The individual sequential images, taken as previously mentioned after each deposition step, allowed the user to determine the order of droplet deposition, which need not be in a strict pattern.

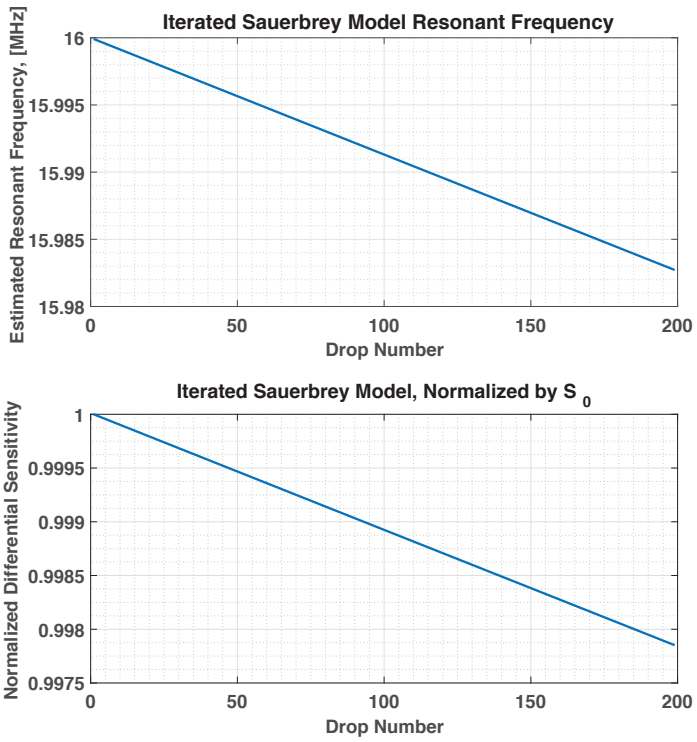

FIGURE 8. Iterated Sauerbrey model evaluated for a 16 MHz CX3225 device (Kyocera) for 6000 pg drop mass. The normalized differential sensitivity is defined as $\frac{1}{S_0}\frac{\Delta f_i}{\Delta m}$.

The individual deposition frequency shifts are plotted in a 3-dimensional scatterbar plot aligned with the drop placement image in order to visualize the relative spatial sensitivity of the device, in Figure 9. As can be seen, the sensitivity is highest in the center of the device's upper electrode, as the drops, which should be of close to uniform mass, produce the highest shift in resonant frequency there.

The absolute sensitivity can be estimated if the drop mass is known. In this case, the average drop mass is 6.1 ng. This drop mass was estimated by deposition of 1,250,000 drops of ink into a clean glass scintillation vial, the mass of which was measured before deposition and after allowing the solvents in the ink to evaporate, computing the differential mass, and dividing by the

number of drops to compute the average drop mass. Therefore the maximum sensitivity of the device can be estimated to be 534 Hz/6100 pg = 0.0875 Hz/pg, but notably this sensitivity rapidly gets significantly worse (close to 0 Hz/pg around the outside of the electrode of the device. The Sauerbrey equation estimated 170 pg/Hz or 0.00588 Hz/pg sensitivity over the entire device, using Equation 3 and the parameters discussed earlier. Thus, it may, in certain sensing applications, be useful to only functionalize the highest sensitivity portions of the device, though whether or not this improves performance will depend on other factors, such as the means by which the sensor is being exposed to the compound or masses to be detected.

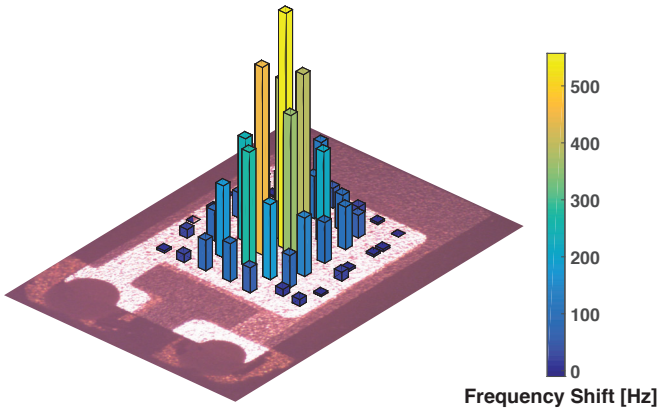

FIGURE 9. Results of a 51-drop experiment compiled into a scatter-bar plot showing the relative frequency shift due to drops in locations across the device.

CONCLUSIONS

An inkjet method for mapping relative mass sensitivity across a resonant structure was successfully developed and applied to a quartz bulk-mode resonator. This method can be used to validate numerical and analytical models employed in design, and also to decide the most promising areas for deposition of functional compounds used in sensing, as long as the drops can be generated in an appropriate size for the application. Future improvements to the process could include refined ink formulation and optimization for the task of keeping spot size small but improve drying times (this could potentially remove the hot air tool from the process). In addition, drop-to-drop variations in mass could cause some error, and characterization of this could be helpful in better bounding the experimental error. Finally, the methodology could be aided by additional automation of the drying system, inkjet system, and back-pressure control to make the characterization a turn-key process.

REFERENCES

[1] O'Toole, R. P., Burns, S. G., Bastiaans, G. J., and Porter, M. D., 1992. "Thin aluminum nitride film resonators: Miniaturized high sensitivity mass sensors". *Analytical Chemistry,* ***64***(11), pp. 1289–1294.

[2] Lee, J. E.-Y., Bahreyni, B., Zhu, Y., and Seshia, A. A., 2007. "Ultrasensitive mass balance based on bulk acoustic mode single-crystal silicon resonator". *Applied Physics Letters,* ***91***(23), p. 234103.

[3] Lee, W. H., Lee, J.-H., Choi, W.-H., Hosni, A. A., Papautsky, I., and Bishop, P. L., 2011. "Needle-type environmental microsensors: Design, construction and uses of microelectrodes and multi-analyte MEMS sensor arrays". *Measurement Science and Technology,* ***22***(4), p. 042001.

[4] Ono, T., Li, X., Miyashita, H., and Esashi, M., 2003. "Mass sensing of adsorbed molecules in sub-picogram sample with ultrathin silicon resonator". *Review of Scientific Instruments,* ***74***(3), pp. 1240–1243.

[5] Stachiv, I., Fedorchenko, A. I., and Chen, Y. L., 2012. "Mass detection by means of the vibrating nanomechanical resonators". *Applied Physics Letters,* ***100***(9), p. 093110.

[6] Tappura, K., Pekko, P., and Seppä, H., 2011. "High-Q micromechanical resonators for mass sensing in dissipative media". *Journal of Micromechanics and Microengineering,* ***21***(6), p. 065002.

[7] Maute, M., Raible, S., Prins, F. E., Kern, D. P., Ulmer, H., Weimar, U., and Göpel, W., 1999. *Sensors and Actuators B: Chemical,* ***58***(13), pp. 505–511.

[8] Thundat, T., Wachter, E. A., Sharp, S. L., and Warmack, R. J., 1995. "Detection of mercury vapor using resonating microcantilevers". *Applied Physics Letters,* ***66***(13), pp. 1695-1697.

[9] Ren, M., Forzani, E. S., and Tao, N., 2005. "Chemical sensor based on microfabricated wristwatch tuning forks". *Analytical Chemistry,* ***77***(9), pp. 2700–2707.

[10] Gupta, A., Akin, D., and Bashir, R., 2004. "Single virus particle mass detection using microresonators with nanoscale thickness". *Applied Physics Letters,* ***84***(11), pp. 1976–1978.

[11] Ilic, B., Yang, Y., and Craighead, H. G., 2004. "Virus detection using nanoelectromechanical devices". *Applied Physics Letters,* ***85***(13), pp. 2604–2606.

[12] Burg, T. P., Godin, M., Knudsen, S. M., Shen, W., Carlson, G., Foster, J. S., Babcock, K., and Manalis, S. R., 2007. "Weighing of biomolecules, single cells and single nanoparticles in fluid". *Nature,* ***446***(7139), pp. 1066–1069.

[13] Nugaeva, N., Gfeller, K. Y., Backmann, N., Lang, H. P., Duggelin, M., and Hegner, M., 2005. "Micromechanical cantilever array sensors for selective fungal immobilization and fast growth detection". *Biosensing and Bioelectronics,* ***21***(6), pp. 849–856.

[14] Raiteri, R., Grattarola, M., Butt, H.-J., and Skladal, P.,

2001. "Micromechanical cantilever-based biosensors". *Sensors and Actuators B: Chemical,* ***79***(2-3), pp. 115–126.

[15] Raiteri, R., Grattarola, M., and Berger, R., 2002. "Micromechanics senses biomolecules". *Materials Today,* ***5***(1), pp. 22–29.

[16] Battiston, F. M., Ramseyer, J. P., Lang, H. P., Baller, M. K., Gerber, C., Gimzewski, J. K., Meyer, E., and Güntherodt, H. J., 2001. "A chemical sensor based on a microfabricated cantilever array with simultaneous resonance-frequency and bending readout". *Sensors and Actuators B: Chemical,* ***77***(12), pp. 122–131.

[17] Kumar, V., Yang, Y., Boley, J. W., Chiu, G. T.-C., and Rhoads, J. F., 2012. "Modeling, analysis, and experimental validation of a bifurcation-based microsensor". *Journal of Microelectromechanical Systems,* ***21***(3), pp. 549–558.

[18] Bajaj, N., Sabater, A. B., Hickey, J. N., Chiu, G. T.-C., and Rhoads, J. F., 2016. "Design and implementation of a tunable, Duffing-like electronic resonator via nonlinear feedback". *Journal of Microelectromechanical Systems,* ***25***(1), pp. 2–10.

[19] Pinnaduwage, L. A., Gehl, A., Hedden, D. L., Muralidharan, G., Thundat, T., Lareau, R. T., Sulchek, T., Manning, L., Rogers, B., Jones, M., and Adams, J. D., 2003. "A microsensor for trinitrotoluene vapour". *Nature,* ***425***(6957), p. 474.

[20] Pinnaduwage, L. A., Boiadjiev, V. I., Hawk, J. E., and Thundat, T., 2003. "Sensitive detection of plastic explosives with self-assembled monolayer-coated microcantilevers". *Applied Physics Letters,* ***83***(7), pp. 1471–1473.

[21] Pinnaduwage, L. A., Hedden, D. L., Gehl, A., Boiadjiev, V. I., Hawk, J. E., Houser, E. J., Stepnowski, S., McGill, R. A., Deel, L., and Lareau, R. T., 2004. "A sensitive, handheld vapor sensor based on microcantilevers". *Review of Scientific Instruments,* ***75***(11), pp. 4554–4557.

[22] García-Romeo, D., Pellejero, I., Urbiztondo, M. A., Ses, J., Pina, M. P., Martnez, P. A., Calvo, B., and Medrano, N., 2014. "Portable low-power electronic interface for explosive detection using microcantilevers". *Sensors and Actuators B: Chemical,* ***200***, pp. 31–38.

[23] Dohn, S., Sandberg, R., Svendsen, W., and Boisen, A., 2005. "Enhanced functionality of cantilever based mass sensors using higher modes". *Applied Physics Letters,* ***86***(23), p. 233501.

[24] Dohn, S., Schmid, S., Amiot, F., and Boisen, A., 2010. "Position and mass determination of multiple particles using cantilever based mass sensors". *Applied Physics Letters,* ***97***(4), p. 044103.

[25] Waggoner, P. S., Varshney, M., and Craighead, H. G., 2009. "Detection of prostate specific antigen with nanomechanical resonators". *Lab on a Chip,* ***9***(21), pp. 3095–3099.

[26] Nieradka, K., Stegmann, H., and Gotszalk, T., 2012. "Focused ion beam milling and deposition techniques in validation of mass change value and position determination method for micro and nanomechanical sensors". *Journal of Applied Physics,* ***112***(11), p. 114509.

[27] Hillier, A. C., and Ward, M. D., 1992. "Scanning electrochemical mass sensitivity mapping of the quartz crystal microbalance in liquid media". *Analytical Chemistry,* ***64***(21), pp. 2539–2554.

[28] Bietsch, A., Zhang, J., Hegner, M., Lang, H. P., and Gerber, C., 2004. "Rapid functionalization of cantilever array sensors by inkjet printing". *Nanotechnology,* ***15***(8), pp. 873–880.

[29] Lang, H. P., and Gerber, C., 2008. "Microcantilever sensors". *Topics in Current Chemistry,* ***285***, pp. 1–27.

[30] Kumar, V., Sabater, A., and Rhoads, J. F., 2011. "Dynamics of coupled electromagnetically-actuated microbeams". The 2011 NSF Engineering Research and Innovation Conference.

[31] Pikul, J., Graf, P., Mishra, S., Barton, K., Kim, Y., Rogers, J., Alleyne, A., Ferreira, P., and King, W., 2010. "High precision polymer deposition onto microcantilever sensors using electrohydrodynamic printing". IEEE Sensors 2010, pp. 2239–2242.

[32] Verkouteren, R. M., Gillen, G., and Taylor, D. W., 2006. "Piezoelectric trace vapor calibrator". *Review of Scientific Instruments,* ***77***(8), p. 085104.

[33] Basaran, O. A., Gao, H., and Bhat, P. P., 2013. "Nonstandard inkjets". *Annual Review of Fluid Mechanics,* ***45***(1), pp. 85–113.

[34] Sauerbrey, G., 1959. "Verwendung von schwingquarzen zur wägung dnner schichten und zur mikrowägung". *Zeitschrift für Physik,* ***155***(2), pp. 206–222.